REPORT DOCUMENTATION PAGE

AFRL-SR-AR-TR-04-

0590

Public reporting burden for this collection of information is estimated to average 1 hour per response, including the time for reviewing ir the data needed, and completing and reviewing this collection of information. Send comments regarding this burden estimate or any c reducing this burden to Washington Headquarters Services, Directorate for Information Operations and Reports, 1215 Jefferson Davis Management and Budget, Paperwork Reduction Project (0704-0188), Washington, DC 20503

1. AGENCY USE ONLY (Leave blank)	2. REPORT DATE 11/11/04	3. REPORT TYPE AND ~~DATES COVERED~~ Final Technical Report 6/01/02 through 11/30/03

4. TITLE AND SUBTITLE	5. FUNDING NUMBERS
An Electromagnetic/Acoustic Propagation Experiment F49620-02-1-0281	
6. AUTHOR(S) H.T. Banks	*F49620-02-1-0281*

7. PERFORMING ORGANIZATION NAME(S) AND ADDRESS(ES)	8. PERFORMING ORGANIZATION REPORT NUMBER
North Carolina State University Center for Research in Scientific Comp. 2610 Stinson Drive Harrelson Raleigh, NC 27695-8205	

9. SPONSORING / MONITORING AGENCY NAME(S) AND ADDRESS(ES)	10. SPONSORING / MONITORING AGENCY REPORT NUMBER
Sharon Heise AFOSR/NM 4015 Wilson Blvd. Rm 713 Arlington, VA 22203	

11. SUPPLEMENTARY NOTES

The views opinions and /or findings contained in this report are those of the author(s) and should not be construed as an official Department of the Army position, policy or decision, unless so designated by other documentation.

12a. DISTRIBUTION / AVAILABILITY STATEMENT	12b. DISTRIBUTION CODE
Approved for public release; distribution unlimited.	

13. ABSTRACT *(Maximum 200 Words)*

We proposed experiments to investigate electromagnetic acoustic waves interaction as part of a technology for pulsed microwave interrogation of materials. The technology involves using reflections of electromagnetic pulses from moving acoustic wavefronts to detect the presence of and determine composition (dielectric and geometric) of hidden objects. Applications of interest to DoD involve non-invasive interrogation of tissue, look-down surveillance and camouflage penetration (e.g., tanks under trees, and subsurface mines and bunkers) and environmental monitoring.

14. SUBJECT TERMS			15. NUMBER OF PAGES 13
			16. PRICE CODE

17. SECURITY CLASSIFICATION OF REPORT Unclassified	18. SECURITY CLASSIFICATION OF THIS PAGE Unclassified	19. SECURITY CLASSIFICATION OF ABSTRACT Unclassified	20. LIMITATION OF ABSTRACT

NSN 7540-01-280-5500

Standard Form 298 (Rev. 2-89)
Prescribed by ANSI Std. Z39-18
298-102

An Electromagnetic/Acoustic Propagation Experiment

AFOSR F49620-02-1-0281

June 1, 2002 – November 30, 2003

Final Technical Report

Prepared by:

H.T. Banks
Center for Research in Scientific Computation
North Carolina State University
Box 8205
Raleigh, NC 27695-8205

20041129 030

TECHNICAL SUMMARY: An Electromagnetic/Acoustic Propagation Experiment

This report represents a summary of our experimental investigations to detect the scattering of microwave frequency electromagnetic waves by induced acoustic structures. The essence of this experiment consists of launching electromagnetic and acoustic waves that will be coincident in a target and observing reflections of the electromagnetic wave in order to detect reflections of the electromagnetic wave off the acoustic wave front. A block diagram of the experimental setup is shown in Figure 1.
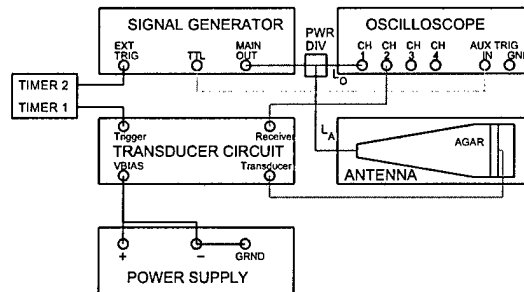

Figure 1: Diagram of the TDR experimental set-up. $L_O = 6$ ft and $L_A = 6$ or 12 ft.

The guiding wave structure is a TEM half plane antenna, as shown in Figure 2. An electromagnetic wave is launched at the feed (narrow end) of the antenna by means of a fast rise-time (200 ps) input pulse from the AVTECH AV-1030-C pulse generator. The TEM antenna guides the spherical wave to the agar target near the aperture (large end) of the antenna. The height and width of the antenna increase from the feed end to the aperture end of the antenna so that the spherical wave approximates a plane wave as it hits the target.
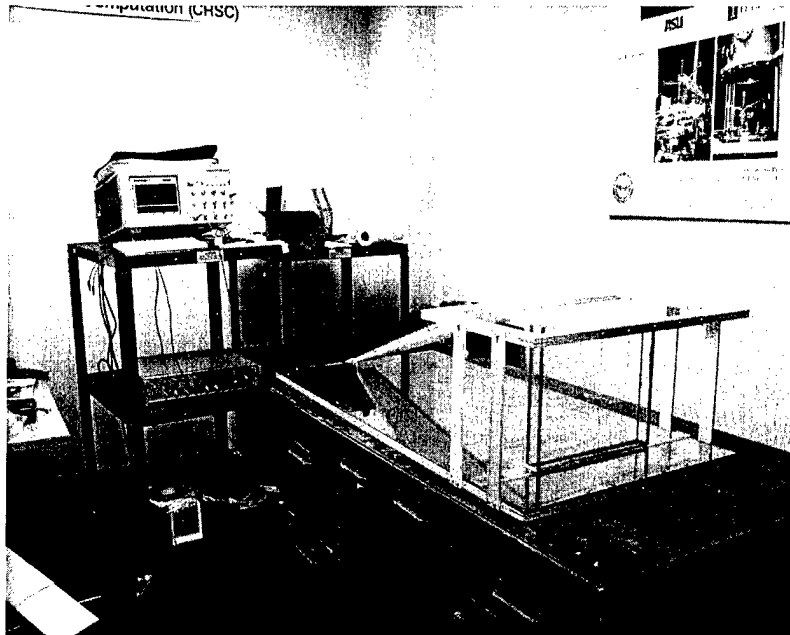

Figure 2: The antenna and some of the related equipment.

Figures 3 and 4 show schematics for the antenna. The ground plane consists of a 1/8 inch thick electronic grade copper plate, while the hot plate (upper triangular plane) is constructed from 100 mesh copper wire cloth and a wooden frame. The agar slab dimensions are $13.00 \times 11.25 \times 1.00$ inches. The outer dimensions of the plexiglass box containing the agar slab are $13.75 \times 12.00 \times 1.75$ inches. A one half inch diameter hole is cut into the center of the back wall (wide end) of the plexiglass container. A hollow plexiglass cylinder ($\frac{3}{4}$ inch length and outer diameter) is centered on the hole and projects out from the container. The acoustic transducer (ITC-215 kHz air transducer) is inserted into the cylinder and and wedged in to make firm contact with the back of the agar slab.
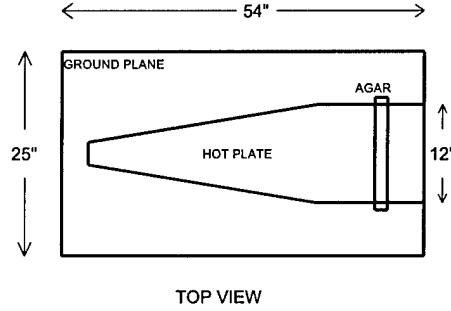

TOP VIEW

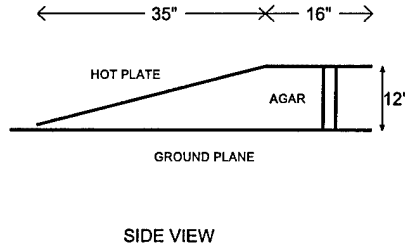Figure 3: Top view of antenna with agar slab (not to scale).

SIDE VIEW

Figure 4: Side view of antenna with agar slab (not to scale).

Time domain reflectometry (TDR) measurements are used to measure the reflections of the electromagnetic wave (from a single input pulse) from structures inside the antenna. To carry out the TDR measurements we used a PE2069 50Ω Resistive Power Divider from Pasternack Electronics. The power divider has a frequency range of DC-6 GHz, an insertion loss of 7 db, and a max VSWR of 1.20:1. The 50Ω power divider splits the signal with minimal reflections.

Referring to the experimental set-up in Figure 1, it can be seen that we measure the incident pulse after the signal is divided and measure the reflected signals that come back from the antenna. These measurements are accomplished using an Agilent Infinium 54854A oscilloscope that is triggered by a TTL signal from the Signal Generator.

EMPTY ANTENNA RESULTS

We first investigated reflections from structures in the antenna in the absence of an acoustic target using TDR measurements. Figure 5 compares data for the two cases of $L_A = 6$ and 12 ft (see Fig. 1). The initial pulses ($t = 0$) for the $L_A = 6$ and 12 ft cases coincide, as expected, representing the portion of the signal generator pulse that travels directly from the splitter to the oscilloscope. The (time) positions of subsequent pulses depends upon the coaxial cable length L_A.

The first reflected pulse occurs at times $t_1 = 19$ and 38 ns for the 6 ft and 12 ft cables, respectively. This

pulse occurs because of reflections at the coaxial cable/antenna connection. The pulse reflected at the coax/antenna junction has the same orientation as the incident pulse. The reflection coefficient is 0.186 (incident voltage/reflected voltage).

The second reflected pulse corresponds to reflections of the transmitted pulse from the end of the antenna. Reflections from the open-ended antenna maintain the same orientation. After the pulse reflects from the end of the antenna a portion is transmitted through the feed to the oscilloscope (incident time $t_2 = t_1 + t_A$), while the rest is re-radiated in the antenna, but with an inverted portion. Subsequent reflected pulses alternate in orientation, each occurs at a time t_A after the next.

This interpretation implies that the reflected signals do not interact with Signal Generator path, but seems to agree well with the data.
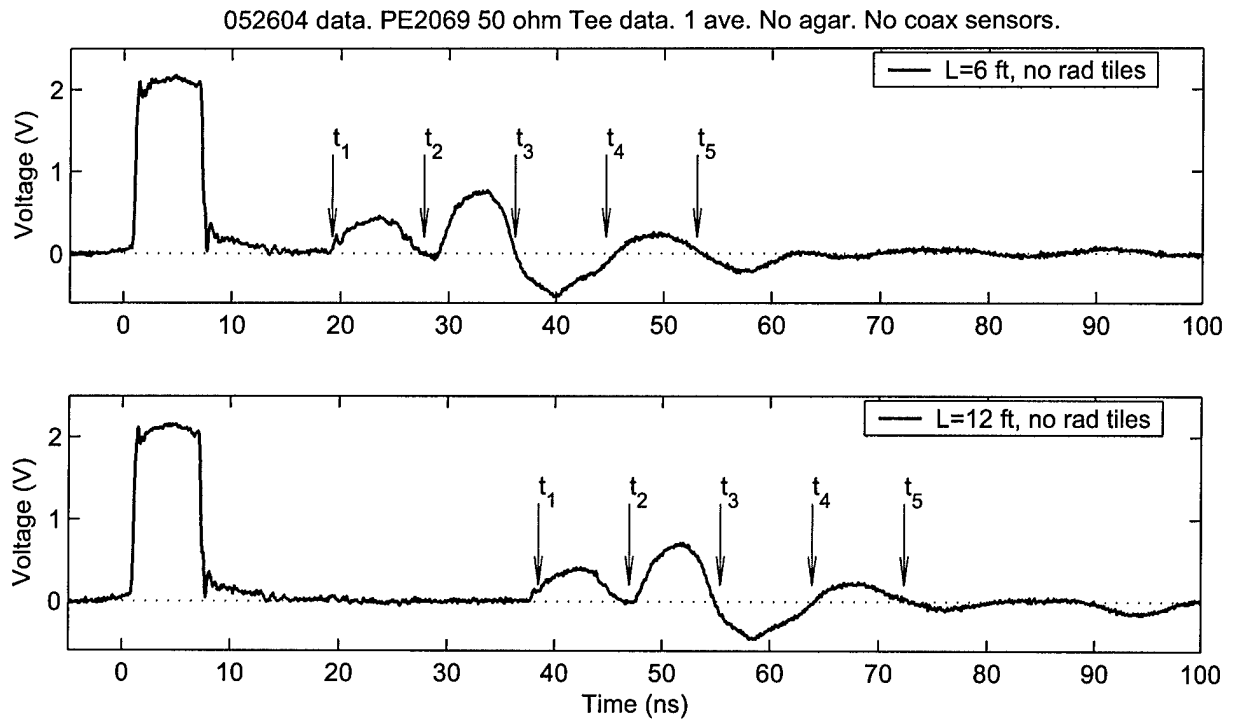

Figure 5: TDR experiment for the two cases of a 6 ft and 12 ft cable from the power divider to the antenna. Calculated reflection times are indicated by the arrows.

Table 2 tabulates the calculated pulse reflection times shown in Figure 5 base upon the interpretation above.

Table 2. *Round-trip Times*

| | CALCULATED REFLECTED PULSE ARRIVAL TIMES | |
	6 ft COAX (ns)	12 ft COAX (ns)
$t_1 = t_{COAX}$	19.25	38.5
$t_2 = t_{COAX} + t_A$	27.71	46.96
$t_3 = t_{COAX} + 2t_A$	36.17	55.42
$t_4 = t_{COAX} + 3t_A$	44.63	63.88
$t_5 = t_{COAX} + 4t_A$	53.09	72.34

Figure 6 compares the reflected pulses with and without absorbing tiles at the end of the antenna. No significant difference can be seen in the two cases. Either the absorption tiles are not doing anything or the reflected and radiated portions are independent.
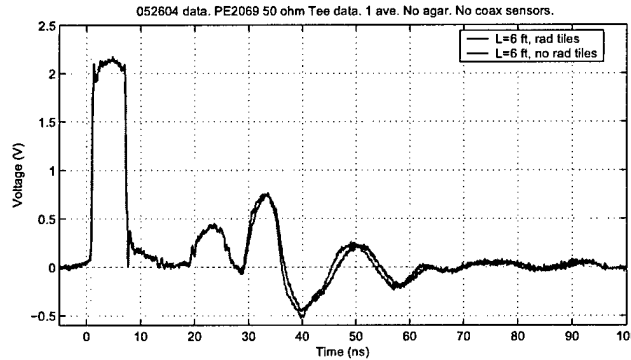

Figure 6: .

RESISTIVE END TERMINATION.

In the next set of experiments we seek to reduce the reflections inside the antenna by varying the end termination at the aperture end of the antenna. Four or five resistors (5% tolerance, 1/4 Watt) are connected in parallel from the hot plate to the ground plane. Figure 7 plots the TDR results for different values of (total) resistance between the hot plate and the ground plane. The first peak in Fig. 7(a) is the (split) pulse directly from the Signal Generator. The second peak is the reflection of the other half of the split pulse at the coaxial cable/antenna feed interface. As expected, this peak is independent of the end termination. The third peak/valley and subsequent features represent repeated reflections of the pulse from the end of the antenna. These features will be greatly affected by the end termination, since reflections from the end of the antenna will be minimized when the end termination resistance matches the characteristic impedance of the antenna at the aperture. From Fig. 7 it is evident that the end reflections are minimized with an end termination of approximately 125 Ω.

These results suggest that the characteristic impedance of the antenna at the aperture end is approximately 125 Ω. The antenna was design to have a 377 Ω characteristic impedance at the aperture in order to be impedance matched to the characteristic impedance of radiation in free space. This design was based on the assumption that the characteristic impedance of the end configuration most closely matched that of a parallel plate configuration (Fig. 8a). Because the ground plane extends out beyond the hot plate, our configuration may more closely resemble that of a microstrip (Fig. 8b). Using the microstrip formula, the characteristic impedance of the antenna at the aperture end ($H = 12$ and $W = 12$ inches) is expected to be $Z_0 = 125\Omega$, which agrees well with the end termination resistance results (above).
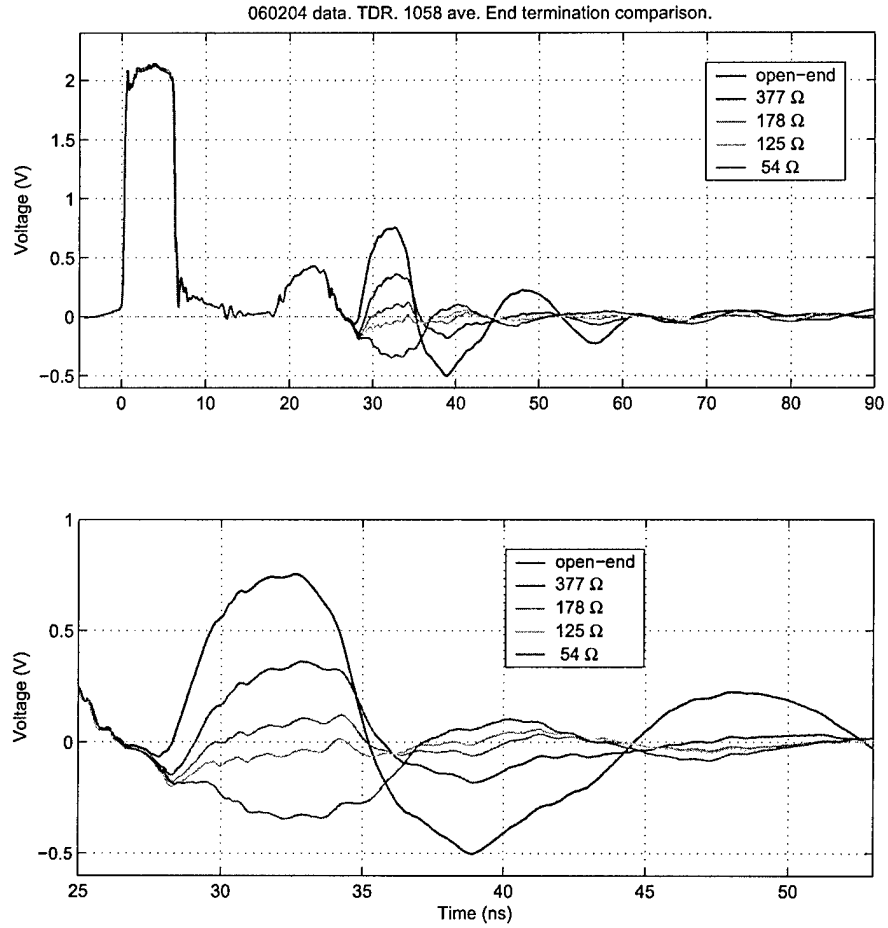
4

Figure 7: TDR results with different resistive end-terminations at the antenna aperture.

CONDUCTOR

$$Z_0 = \eta \; H/W$$

(a) Parallel Plate.

TOP CONDUCTOR   **FRINGING FIELD**

$\leftarrow$ **W** $\rightarrow$

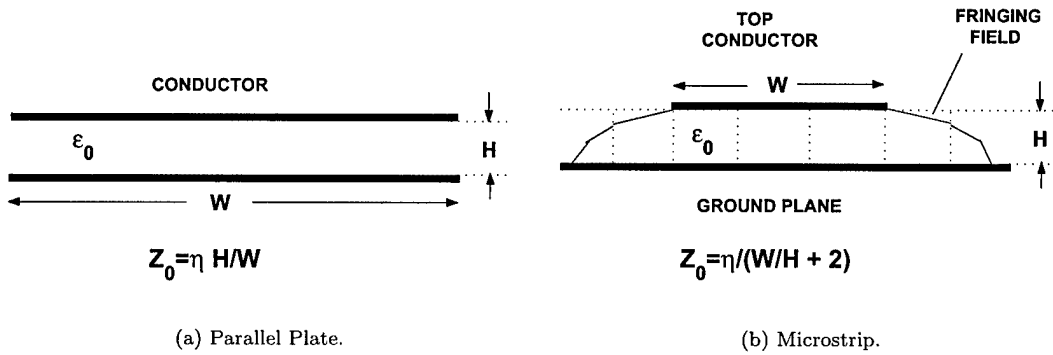**GROUND PLANE**

$$Z_0 = \eta/(W/H + 2)$$

(b) Microstrip.

Figure 8: Two different configurations that approximate the characteristic impedance of the antenna at the aperture end The dimensions of the antenna are $H = 12$ and $W = 12$ inches at the aperture. In the equations $\eta = \sqrt{\mu_0/\epsilon_0} = 377\Omega$ is the characteristic impedance of free space.

TRANSDUCER CHARACTERIZATION

The ultrasonic transducer also acts as a receiver of acoustic waves. The receiver capability can be used to

5

check that the transducer is functioning properly and to measure the velocity of sound in the agar target. Figure 9 plots the signal that is received by the transducer as a function of time for different target distances (D). The initial portion of the signal is the same for all cases and represents the ring-down of the pulse in the transducer. The secondary pulses represent the reflection of the acoustic signal from a hard target. As expected, the locations (round-trip times) of the reflected pulses increase as the target distance increases.
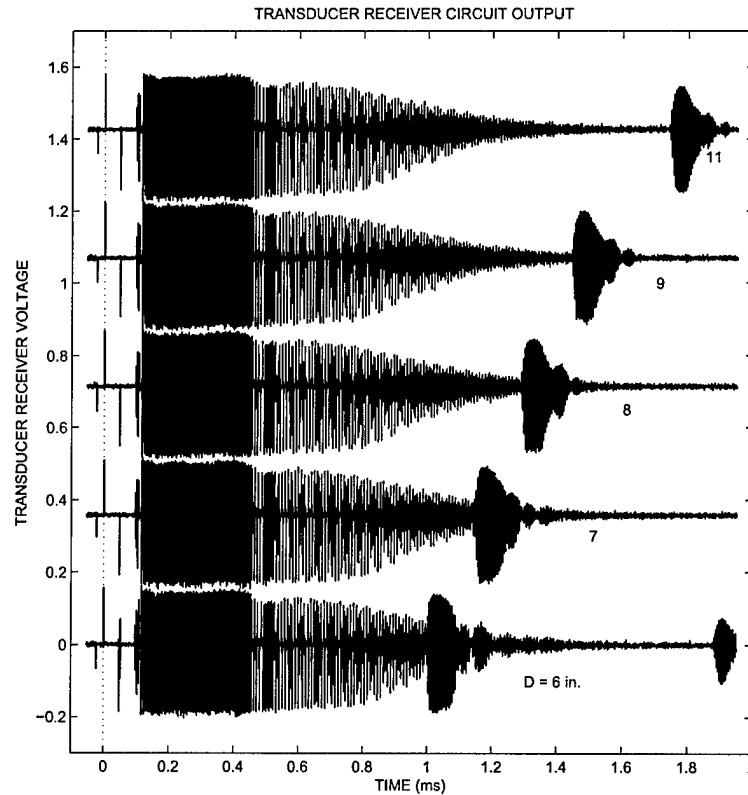
Figure 9: Output of the received transducer signal (Volts) as a function of time for different target distances (D).

The time of arrival of the reflected pulse is plotted as a function of the target distance in Figure 10 (circles) along with the calculated round-trip time (line). Offsetting the calculated times by 0.11 ms gives good agreement between the observed and calculated arrival times. The offset time probably represents a fixed delay time in the circuit.
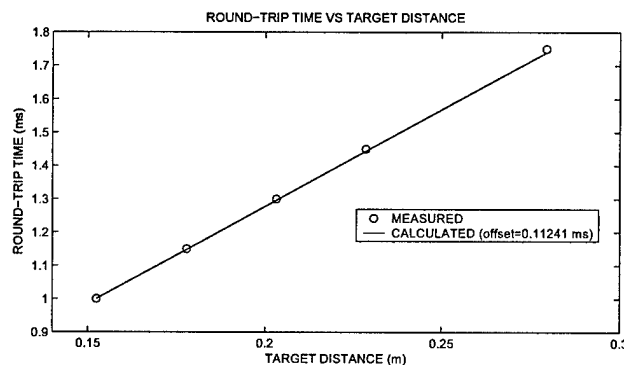

Figure 10: Observed (circles) and calculated (line) arrival times for the reflected acoustic pulses as a function of the target distance D.

MEASUREMENT OF THE VELOCITY OF ACOUSTIC WAVES IN AGAR

To measure the velocity of the acoustic waves in agar we mount the transducer on the top (narrow) surface of agar and point it down into agar. The acoustic pulse travels 0.29 m to the bottom plexiglass surface, where it is reflected back to the transducer. The reflected signal received by the transducer is shown in Figure 11 (black curve). The initial portion of the signal (0-0.5 ms) represents the ring-down period of the transducer receiver circuit. There are many oscillations in the signal from the receiver circuit, but distinct reflection "pulses" are evident. It is easier to look at a min/max smoothed plot of the data shown above.
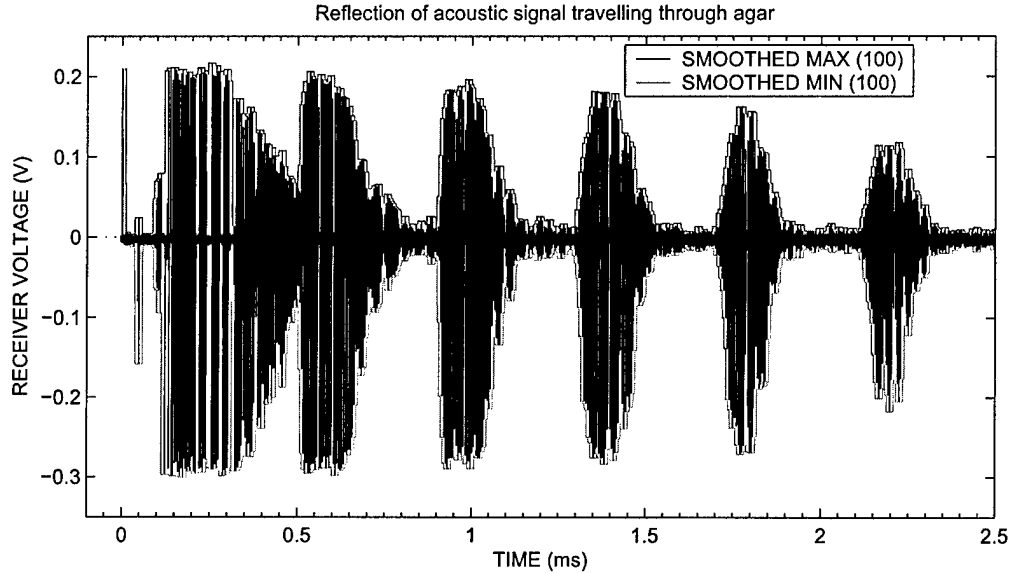

Figure 11: Oscilloscope measurement of transducer receiver circuit signal for the case of an acoustic wave travelling through agar. Reflections from the opposing plexiglass surface can be seen at 0.5 ms and at approximately 0.4 ms intervals thereafter. The red and green curves show the min/max smoothed curved for this data ($N = 100$).

At each time point the plotted value equals the maximum (red curve) or minimum (green curve) value of the current point and N points ahead and behind the current point (Figure 12 with $N = 100$). The velocity of the acoustic wave in agar is calculated to be the round-trip distance in agar divided by the time between reflections. Here the velocity is measured to be 1450 m/s, which is consistent with published values.

COMPARISON OF THE TRANSDUCER RECEIVER SIGNAL IN AIR AND AGAR

The transducer is mounted against the back of the agar as is the case when measuring EM/Acoustic interactions. The acoustic pulse travels 1 inch before reflecting from the opposing plexiglass surface. The transducer is aimed at a distant point outside the antenna (in air). No reflections are evident in the air, because of the large distance. The reflections in agar are spaced at 50 μs intervals. The spacing should be 35 μs.
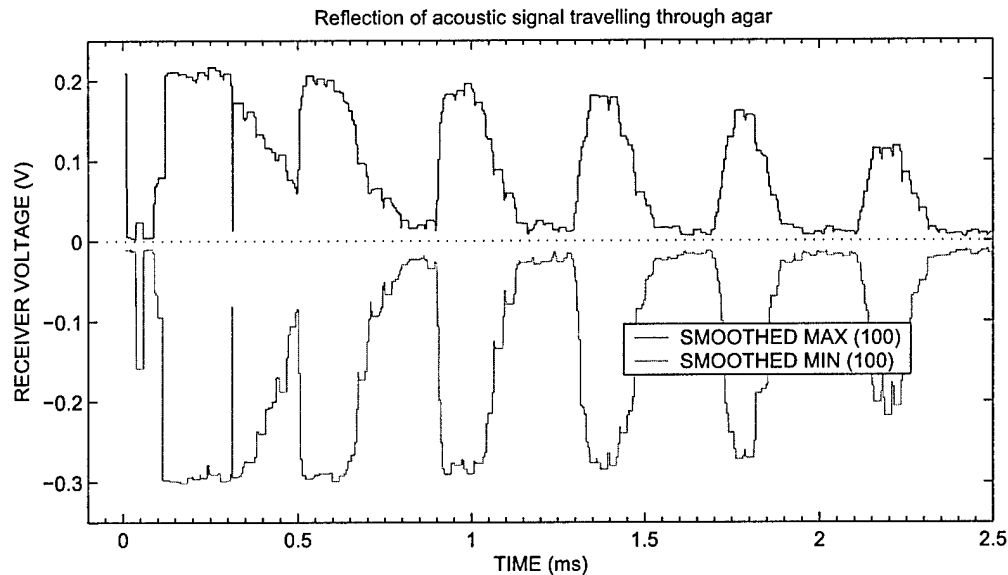
Figure 12: The min/max smoothed plot of the signal from the transducer receiver circuit showing reflections of the acoustic pulse from the plexiglass surface.
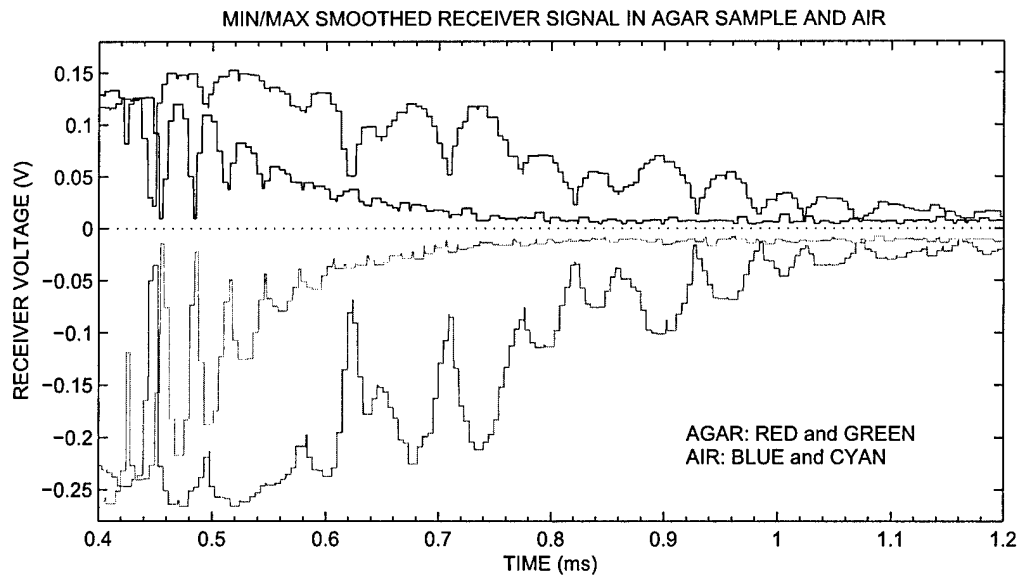

Figure 13: The signal from the transducer receiver circuit for a pulse traveling in air (blue and cyan curves) as compared to a pulse traveling in the agar (red and green curves).

SYNCHRONIZATION OF EM AND ACOUSTIC WAVES

In order to have the electromagnetic and acoustic waves coincident in the antenna we must have allow a sufficient delay for launching the electromagnetic wave after the acoustic wave is launched, since the velocity of the electromagnetic wave is much greater than that of the acoustic wave. The synchronization is accomplished with two timer circuits and a variable delay time control on the Signal Generator. The first timing circuit triggers the second timing circuit as well as providing the trigger input for the transducer circuit. The second triggering circuit serves as an external trigger to the Signal Generator. Synchronization of the acoustic and EM pulses is achieved by selecting an appropriate value for the delay time on the Pulse

Generator. The delay time is the time between the arrival of the External Trigger pulse and the output of the EM pulse from the Pulse Generator (Fig. 14). [1] The experimental setup with the timing circuits is shown in Figure 1.
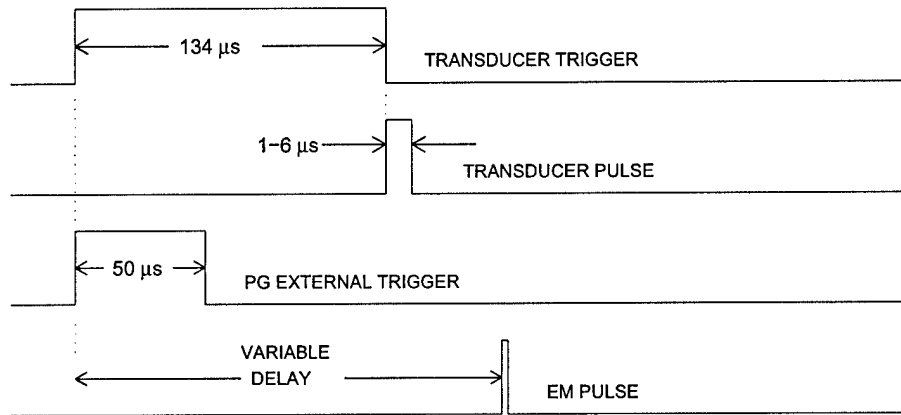

Figure 14: Schematic diagram of the signal timing.

EM/ACOUSTIC DATA - MEASUREMENTS WITH DIFFERENT DELAYS

We next perform TDR experiments with an agar target and acoustic waves. We vary the delay time to sample a range of possible positions of the acoustic wave in the agar at the time of incidence of the EM wave. Figure 15 plots the positive portions of the transducer receiver signals for the different delay times that were used. Time $t = 0$ indicates the (relative) time at which the EM wave is launched in the antenna.
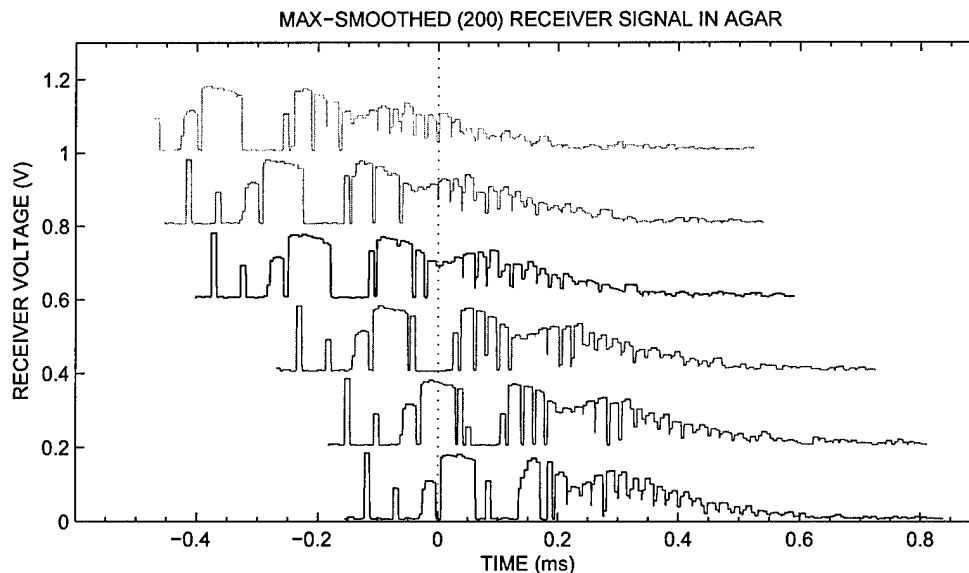

Figure 15: .

The TDR measurements for the different delay times are plotted in the upper half of Figure 16. Because of reflections from other structures in the antenna, reflections of the EM wave off the acoustic wave structure,

---

[1]More accurately, the Delay Time is the time between output of the SYNCH pulse and output of the EM pulse. There is a fixed propagation delay of 60 ns between the External Trigger and SYNCH pulses.

if they exist, are expected to be small in comparison. For this reason we plot a subtracted signal in the lower half of Figure 16. The subtracted signal is the difference between TDR measurements with and without an acoustic wave in the agar target.
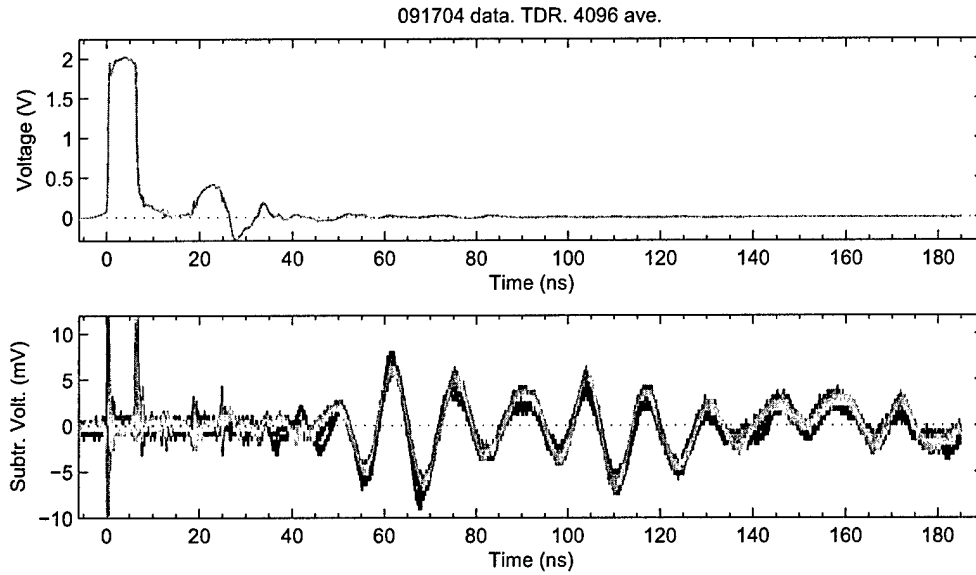

Figure 16: .

Figure 17 provides a close look at the above plot in the time region where we expect the EM and acoustic waves to be first coincident, for the different delay times.
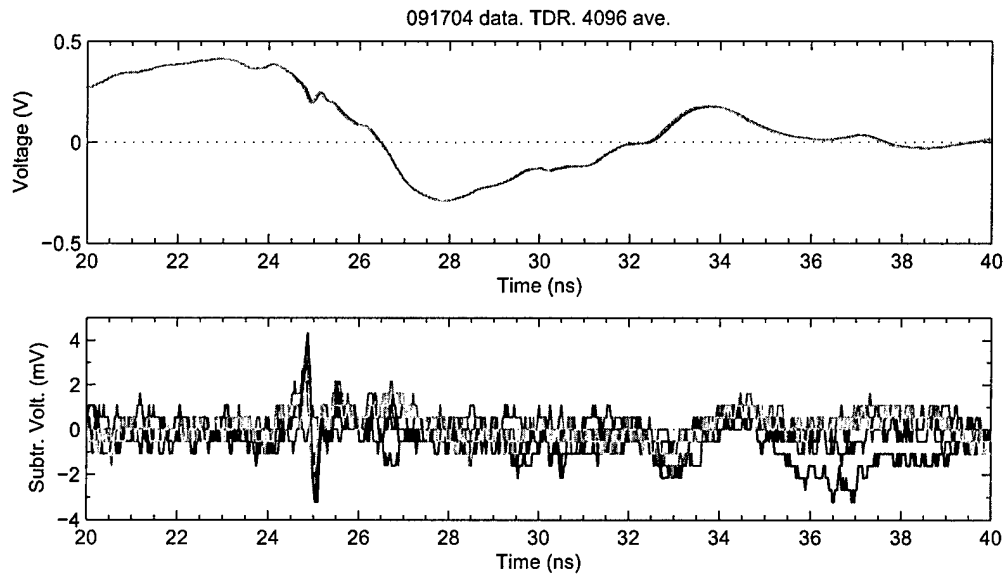

Figure 17: .

In Figure 18 we take a closer look at the variability in the input pulse width, as evidenced by the positive and negative spikes at the leading and trailing edges of the input pulse.
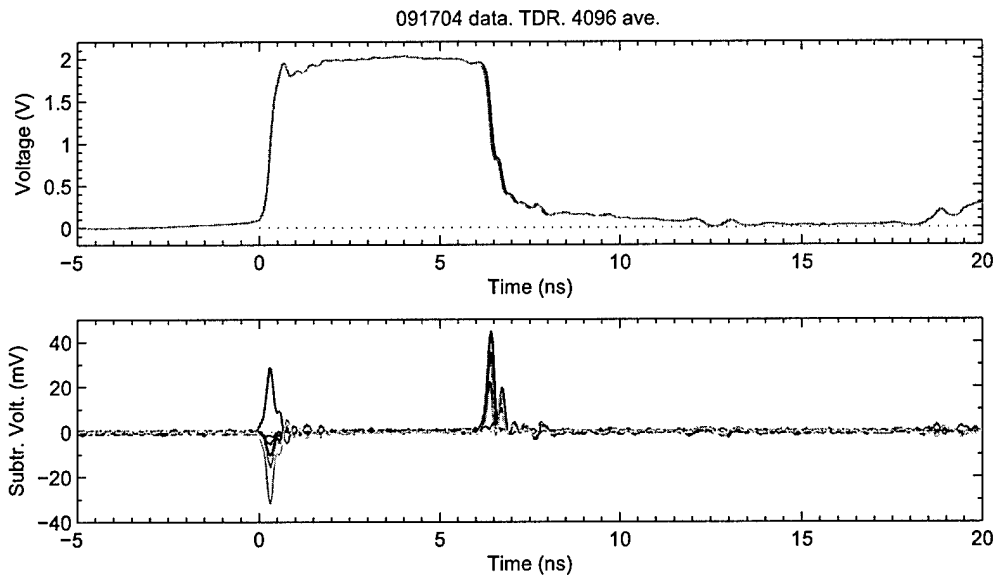
091704 data. TDR. 4096 ave.

Figure 18: .

SUMMARY

In summary, we have constructed a workable antenna where we can launch EM waves at the agar target and make TDR measurements. The circuitry and timing necessary to initiate an acoustic wave and synchronize it with the EM pulse has been built. We have carried out TDR experiments and have observed differences in the case when there is an acoustic wave in the agar. We are in the process of investigating these differences to determine whether they are the result of EM reflections from the acoustic wave front. In addition to the TDR measurements, future work can include other sensing equipment, such as an electric field sensor or a Ddot probe.